High Temperature Brazing by Liquid Infiltration

Liquid infiltration reduced the intermetallic forming elements and improved the mechanical properties of brazements with large joint clearances

BY W. D. ZHUANG and T. W. EAGAR

ABSTRACT. High temperature brazing of nickel-based alloy Inconel[1] 625 by liquid infiltration has been investigated. Nickel-phosphorus, nickel-boron and Ni-41.2Pd-8.8Si were used as melting point depressants (MPDs). They formed wetting liquids at the bonding temperature and subsequently infiltrated the nickel-chromium powder interlayers. The infiltrated liquid caused shrinkage of the powder interlayer. Calculation showed that residual porosity in the interlayer was related to its initial green density, the amount of liquid and a shrinkage factor. Liquid infiltration greatly reduced the necessary amount of intermetallic forming elements such as phosphorus and boron in the joints, thereby improving the mechanical properties of brazements with large joint clearances. Joints with clearance up to five millimeters (0.2 in.) have been made. Tensile strengths at room temperature, 538°C (1000°F) and 700°C (1300°F) were evaluated.

Introduction

Nickel-based filler metals have been widely used in brazing processes to produce oxidation and corrosion-resistant, high-strength joints for high/temperature service. These filler metals usually contain several MPDs, such as silicon, boron and phosphorous to ensure proper liquid flow and wetting at the brazing temperature. However, these elements can form eutectic structures that are extremely hard and brittle in the brazed joint. These appear as hard phases in the form of silicides, borides and phosphides. These phases often agglomerate along the centerline of the joint and can greatly decrease the strength and ductility of the joint. Consequently, the maximum joint clearance that is free of intermetallic compounds is generally restricted to less than several tens of microns when nickel-based filler metals are used (Refs. 1–7). Post-brazing high temperature annealing can help to partially dissolve or eliminate the intermetallics and improve the mechanical properties of the joint. Such beneficial effects also can be accomplished by diffusion brazing, which has been successfully applied in joining some heat resistant superalloys (Refs. 8–11). Instead of cooling down the joint after liquid flow during brazing, the joint is held at the joining temperature for solidification by the diffusion brazing process. Isothermal holding makes the MPDs diffuse into the base material and a joint free of brittle intermetallics can be made. However, tens of hours of isothermal holding is generally required to allow solid state diffusion of the MPDs into the base material (Refs. 12, 13). Therefore, a practical solidification time for the diffusion brazed joint also imposes restrictions on the maximum joint clearance that can be used.

In this study, a process called liquid infiltrated powder interlayer bonding (LIPB) is used to produce brazements with large joint clearances using nickel-based filler metals. The filler metals consist of coatings and thin foils on the faying surfaces. A powder interlayer is placed between the two fillers. At brazing temperature, the fillers melt and infiltrate the powder interlayer. Dissolution and rearrangement of powder particles occur subsequently, followed by homogenization of the joint. By controlling the amount of liquid formed, brittle phases and porosities in the powder interlayer can be reduced to a minimum, while a clearance of up to several millimeters can be joined. Isothermal solidification time is much shorter as compared to the diffusion brazing process since the diffusion path is greatly decreased in the powder interlayer. Thus the LIPB process relaxes the limitation on joint clearance set by the diffusion brazing process.

KEY WORDS

High-Temp. Brazing
Liquid Infiltration
Powder Interlayer
Bonding
Joint Clearance
Nickel-Based Alloys

General Considerations of the LIPB Process

One of the ways to decrease the amount of brittle intermetallic compounds in the joint is to reduce the MPDs used to produce the joint. This may be achieved via the LIPB process. The process can be divided into four consecutive stages, which are illustrated in Fig. 1, or represented in a simple binary eutectic phase diagram as seen in Fig. 2. The important parameters of the process can be derived based on such a binary system. Assuming that the powder interlayer has the same MPD composition as the base metal, $C_B{}^i$ and $C_B{}^o$ denote the base metal concentration in the infiltrant and overall base metal concentration in the joint, respectively. At the bonding temperature T_b, liquid starts to form as the MPDs dis-

W. D. ZHUANG and T. W. EAGAR are with the Department of Materials Science and Engineering, Massachusetts Institute of Technology, Cambridge, Mass.

Paper presented at the 26th International Conference on Brazing and Soldering, AWS Annual Convention, Cleveland, Ohio, April 1995.

1. Inconel is trademark of the Inco family of companies.

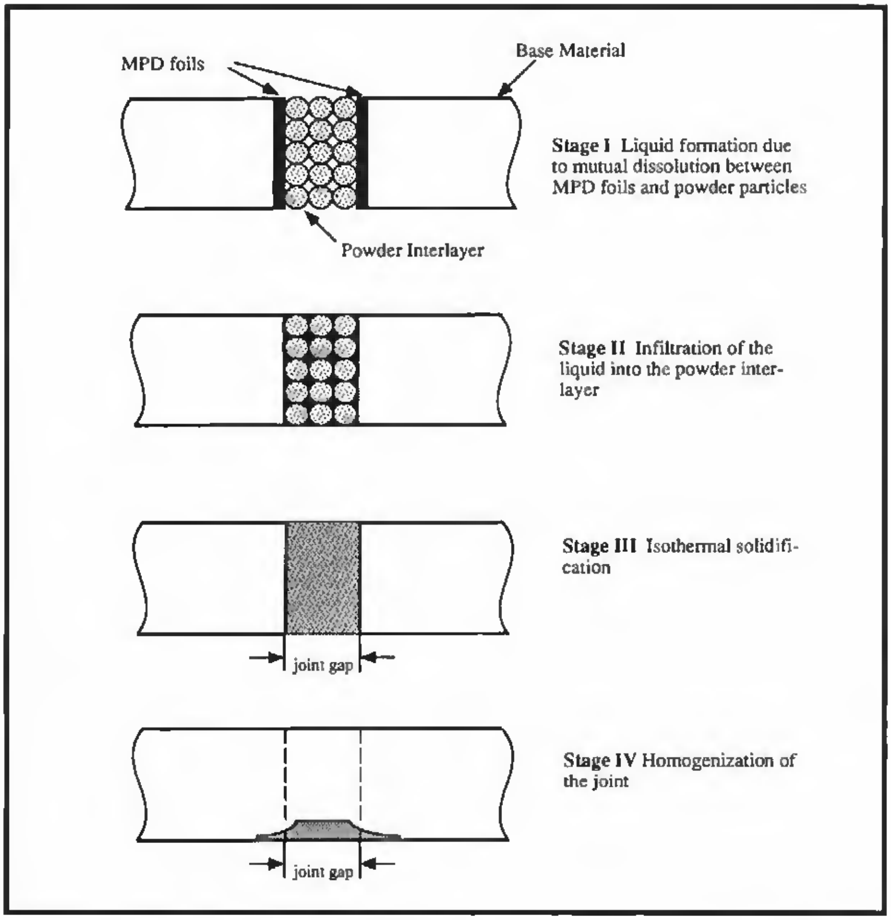

Fig. 1 — Schematic showing the stages of the LIPB process. The widening stage is absent since the dissolution mainly occurs between the powders and the MPD foils. The stages may overlap depending on the rates of infiltration and diffusion.

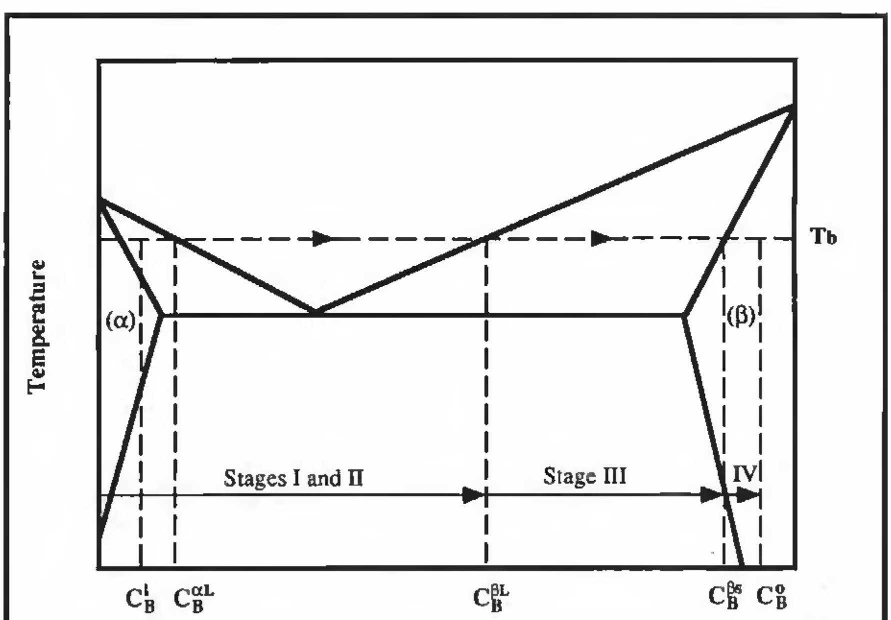

Fig. 2 — Schematic drawing of a phase diagram shows a simple eutectic reaction between the melting point depressant and the powder particles. C denotes the base metal concentration in the diagram. Four stages of the LIPB process also are illustrated.

solve the base material and change its composition to $C_B^{\alpha L}$. The wetting liquid infiltrates the powder interlayer while dissolving more base material until the composition of the liquid changes to $C_B^{\beta l}$, which corresponds to the maximum amount of liquid formed. Shrinkage of the interlayer is induced by the infiltrated liquid and the joint undergoes solidification between $C_B^{\beta l}$ and $C_B^{\beta s}$, followed by homogenization of the joint. An analysis of the residual porosity in the interlayer is derived here under the assumptions of complete wetting and spontaneous infiltration. Base metal-MPD intereaction is not considered because of fast infiltration kinetics and rapid intereaction between the liquid and the metal powders in the interlayer. The initial relative density of the powder interlayer is Δ_o with a thickness of t_o, and A is the cross-sectional area of the interlayer. Assuming uniform dissolution of the powder interlayer, when the infiltrant is unsaturated ($C_B^i < C_B^{\beta L}$) and neglecting the MPD loss by solid state diffusion into the base material, then the weight of powders of the interlayer dissolved in the liquid is:

$$W_{base}^{L} = W_{MPD}\left(\frac{C_B^{\beta L}}{1-C_B^{\beta L}} - \frac{C_B^{i}}{1-C_B^{i}}\right) \tag{1}$$

where W_{MPD} is the total weight of MPDs in the joint. The volume of liquid is given by

$$V^{L} = W_{MPD}\left(\frac{C_B^{\beta L}}{\rho_L\left(1-C_B^{\beta L}\right)} + \frac{1}{\rho_L}\right) \tag{2}$$

where ρ_L is the density of the liquid. Correspondingly, the volume of the remaining solid in the joint is:

$$V^{s} = \frac{W_{base}}{\rho_s} - \frac{W_{MPD}}{\rho_s}\left(\frac{C_B^{\beta L}}{1-C_B^{\beta L}} - \frac{C_B^{i}}{1-C_B^{i}}\right) \tag{3}$$

where ρ_s is the density of the base material. The W_{MPD} can be represented by the overall composition of the base material in the joint, C_B^o:

$$W_{MPD} = A\,\rho_s \Delta_o t_o\left(\frac{\left(1-C_B^{i}\right)\left(1-C_B^{o}\right)}{C_B^{o}}\right) \tag{4}$$

The weight of the powder interlayer, W_{base}, is given by

$$W_{base} = A\,\rho_s \Delta_o t_o \tag{5}$$

Assuming no swelling or shrinking of the powder interlayer after infiltration, the residual volume fraction of porosity after infiltration can be expressed as:

$$P = 1 - \frac{V^s + V^l}{A\, t_o} \qquad (6)$$

Substituting equations 1 through 5 into 6, one finally arrives at

$$P = 1 - \Delta_o \left[1 - \frac{\left(1 - C_B^o\right)\left(C_B^{\beta L} - C_B^i\right)}{C_B^o\left(1 - C_B^{\beta L}\right)} + \frac{\rho_s\left(1 - C_B^o\right)\left(1 - C_B^i\right)}{\rho_L C_B^o\left(1 - C_B^{\beta L}\right)} \right] \qquad (7)$$

If assuming the same density of liquid and solid, Equation 7 reduces to:

$$P = 1 - \frac{\Delta_o}{C_o} \qquad (8)$$

Apart from the calculation above, the powder interlayer can experience additional volume change due to infiltration of the liquid. A constant k is introduced to account for this additional volume change:

$$P = 1 - \frac{\Delta_o}{C_o} \qquad (9)$$

k<1 indicates shrinkage of the powder interlayer and k>1 represents swelling. Obviously, higher initial relative density and lower C_B^o will lead to a denser joint. However, in order to maintain acceptable mechanical properties of the joint, C_B^o is required to be as high as possible. Tradeoffs exist between the higher MPD concentration or larger volume fraction of residual porosity in the joint. A TLP joint requires C_B^o greater than $C_B^{\beta s}$ as illustrated in Fig. 1. If we set $C_B^o = C_B^{\beta s}$, then the minimum initial relative density of the powder interlayer needed for a porosity free joint is:

$$\Delta_o = k\, C_B^{\beta s} \qquad (10)$$

It is evident that smaller k, lower $C_B^{\beta s}$ or higher solubility of MPDs in the base metal will allow lower initial packing density of the powder interlayer, which will be easier to infiltrate. Nevertheless, as has been pointed out in Ref. 14, diffusional solidification can block the infiltrating liquid if the solubility of MPDs in the base material is high. Therefore, the infiltration rate can be retarded significantly because of the solubility effect, as will be shown in our experiments.

Table 1 — Chemical Compositions of the Infiltrants Used (wt-%)

Materials	Pd	Si	P	B	Ni	Solidus (°C)	Liquidus (°C)
Ni-P	—	—	11	—	Bal.	870	870
Ni-B	—	—	—	3.6	Bal.	1093	1093
MBF-1006	41.2	8.8	—	—	Bal.	714	938

Table 2 — Chemical Compositions of the Base Metals Used (wt-%)

Materials	C	Mn	P	Si	Cr	Cu	Mo	Ti	Nb	Fe	Al	Co	Ni
Nickel	0.01	0.2	—	0.04	—	—	—	—	—	0.15	—	—	Bal.
Inconel 625	0.04	0.11	0.01	0.36	22.6	0.18	8.85	0.25	3.68	4.99	0.16	0.2	Bal.

Experimental Work

Materials

The infiltrants selected for this investigation were Ni-P eutectic, Ni-B eutectic and Ni-41.2Pd-8.8Si (MBF-1006) alloys. The chemical composition of the infiltrants used are given in Table 1 with their solidus and liquidus temperatures. The base metal studied was commercially pure nickel and Inconel 625 nickel-based alloy. The powders investigated were commercially pure nickel and Ni-20wt-%Cr powders with sizes less than 44 microns (–325 mesh). The chemical composition of the base metals used is shown in Table 2.

LIPB Procedure

The Ni-P and Ni-B eutectics were electrolessly plated onto the faying surfaces according to Riedel (Ref. 15), whereas the silicon-containing alloy is in the form of thin amorphous foils. The powder interlayers were all prepared in a 9.55-mm-diameter cylindrical die at 373 MPa compressive pressure. The green density of the interlayers was found to be about 72% by volume. The faying surfaces of the butt joints were polished to 600 grit paper and were ultrasonically cleaned in acetone before joining.

Bonding was performed in a quartz tube resistance furnace. The furnace was first evacuated to 2.7 x 10^{-3} Pa (2 x 10^{-5} torr), and preheated to 900°C (1652°F) before it was placed on the sample. The joining temperature was 980°C (1796°F) for the nickel-phosphorus, 1000°C (1832°F) for the MBF-1006 and 1125°C (2055°F) for the nickel-boron eutectic. The average heating rate for joints using Ni-P and MBF-1006 as infiltrants was 20°C (68°F)/min. The rate was dropped to about 14°C (57°F)/min for the boron-containing joints. During joining, a minor pressure of about 0.29 MPa (41 lb/in.^{2}) was applied on the sample to ensure close contact of the fillers and the powder interlayer. Each joint was cut for metallographic examination. Standard round tensile specimens, each with a 6.0-mm-diameter cross section, were made to evaluate tensile strength of the joints. Room temperature, 538°C (1000°F) and 700°C (1300°F) strengths were evaluated.

Results and Discussion

Microstructures

Figure 3A shows the microstructure of a joint with 0.6-mm clearance using nickel as the base metal. About 50 microns of Ni-P eutectic was plated on each of the faying surfaces, and nickel powders were used to form the interlayer. Joining was performed at 980°C for 60 min. The joint can be seen to have completely homogenized. The overall phosphorus content in the joint after infiltration was 2.4 wt-%, which is more than four times lower than in commercially available brazing alloys BNi-6 and BNi-7. In Fig. 3B, the same joining conditions — except a 1.5 mm powder interlayer — were applied to make the joint. The powder interlayer was not fully infiltrated, leaving a narrow uninfiltrated zone in the center of the interlayer. Calculation from Equation 10 indicates k<1 for infiltration using Ni-P eutectic, thus liquid-induced shrinkage of the powder interlayer helped to eliminate the voids. It can be estimated from Fig. 3B that the minimum phosphorus content achievable in the joint through the LIPB process is about 1.8 wt-%, and in fact this criterion was applied for all subsequent joints that were infiltrated by Ni-P eutectic.

Figure 3C is the microstructure of MBF-1006 infiltrated joint. The 0.65-mm-thick interlayer consisted of nickel

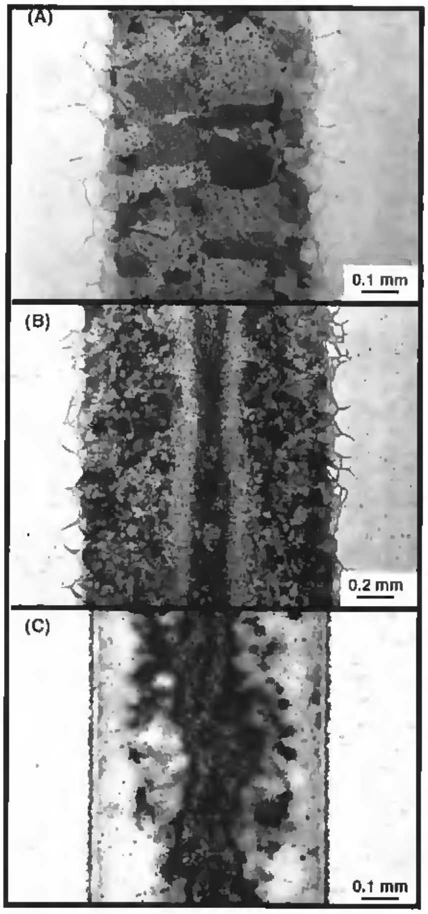

Fig. 3 — Microstructures of infiltrated joints. A — 0.6-mm nickel powder interlayer infiltrated by Ni-P eutectic at 950°C for 60 min. The base metal is nickel and the phosphorus content in the joint is 2.4 wt-%. B — Same as A, only the interlayer is increased to 1.5 mm. C — 0.65-mm nickel powder interlayer infiltrated by MBF-1005 at 1000°C for 30 min. The base metal is Inconel 625 and the designed silicon content is 2 wt-%.

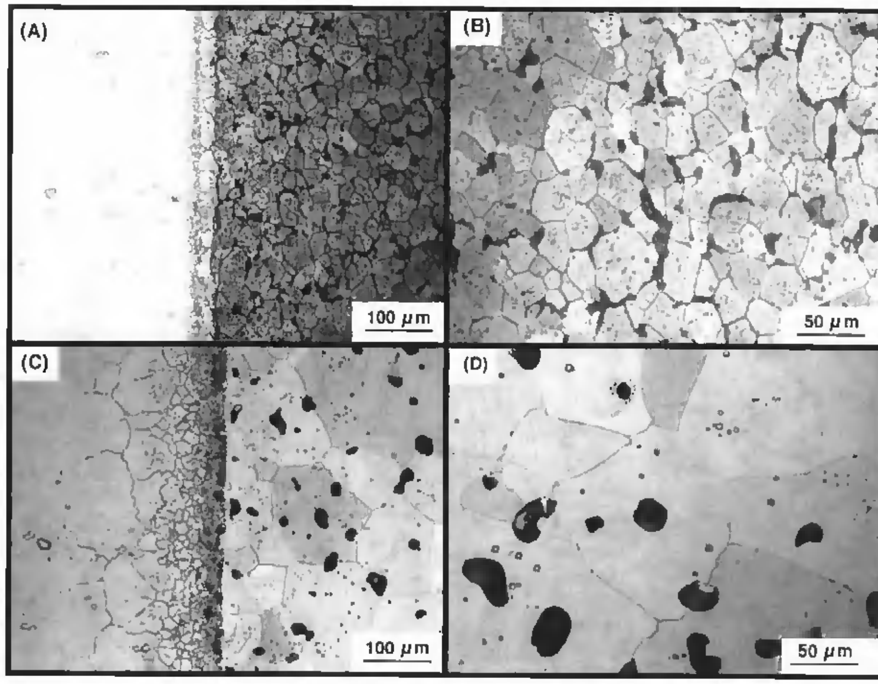

Fig. 4 — Microstructures of infiltrated joints with 3.54-mm-thick Ni-20Cr powder interlayers. A — Interface between Inconel 625 and the powder interlayer infiltrated by Ni-P eutectic at 980°C for 60 min. B — Same as A, microstructure of the interlayer. C — Ni-B eutectic as the infiltrant, 1125°C, 60 min infiltrated. D — Microstructure of the interlayer.

powders. Infiltration was performed at 1000°C for 30 min. The designed silicon content in the joint was 2 wt-%, which is below the solubility limit of silicon in nickel (about 7 wt-% at 1000°C). Only partial infiltration of the powder interlayer was obtained. The lower infiltration rate is likely due to large solubilities of palladium and silicon in nickel. Diffusional solidification occurs along with the infiltrating liquid, and consumes the liquid before the entire interlayer is infiltrated.

Figures 4A and 4B are the microstructures of a Ni-P eutectic-infiltrated joint with 3.54-mm Ni-20Cr powder interlayer. The joint was soaked at 980°C for 60 min. Figure 4A shows the interface between the Inconel 625 base metal and the Ni-20Cr powder interlayer. The microstructure of the interlayer after infiltration is shown in Fig. 4B. Note that oxides from the powder surfaces are trapped in the grain boundaries. Figures 4C and 4D show the microstructures of Ni-B eutectic-infiltrated joint at 1125°C for 60 min. The same 3.54-mm Ni-20Cr powder interlayer was used and the designed boron content in the joint was 0.33 wt-%. Deeper penetration of boron into the Inconel 625 base metal can be seen as compared to that of phosphorus. This was due to the higher diffusivity of boron and the higher temperature employed to produce the joint. Significant grain growth can be seen in Fig. 4D, and a large amount of isolated pores remains in the joint. It turned out that the effect of powder interlayer shrinkage was insignificant when using the Ni-B eutectic infiltrant. Higher green density of the interlayer and/or more infiltrant should be used to eliminate residual pores in this sample.

Tensile Tests

Figure 5 shows the tensile properties of the LIPB joints using Ni-P eutectic as the infiltrant and 3.54-mm-thick Ni-20Cr as the interlayer. Tensile strength of the joints infiltrated by Ni-B eutectic is presented in Fig. 6. For the joints infiltrated by Ni-P eutectic, their room temperature, 538°C, and 700°C strengths were evaluated. Two specimens were used for testing at each temperature. Consistent tensile strength was observed for each group of specimens tested. The average room temperature strength was 523 MPa (75 ksi). The 538°C strength decreased to 420 MPa (57 ksi) and the average strength dropped to 300 MPa when tested at 700°C. The data showed about 60% of the Inconel 625 base metal strength within this temperature range. However, the tensile strength was found to be much lower for the joints infiltrated by Ni-B eutectic at 1125°C. All the specimens tested were found to fracture in the powder interlayer, as shown in Fig. 6A, indicating strong interfacial bonding between the interlayer and the base metal. Figures 6B and 6C show the fracture surfaces of the room-temperature tested sample with Ni-P as the infiltrant. Apart from the effect of the MPDs, the interlayer strength also could be impaired by the oxides distributed on the surfaces of the alloy powders. A powder cleaning procedure before joining may improve the interlayer strength. The ductility of the joints is still much lower than that of the base metal, although plastic deformation was observed. This is due to a large amount of phosphorus (1.8 wt-%) left in each joint, although phosphides are not discernible from the microstructures shown here.

As can be expected from the microstructures revealed in Figs. 4C and 4D, the tensile strength of Ni-B eutectic infiltrated joints is degraded by the presence

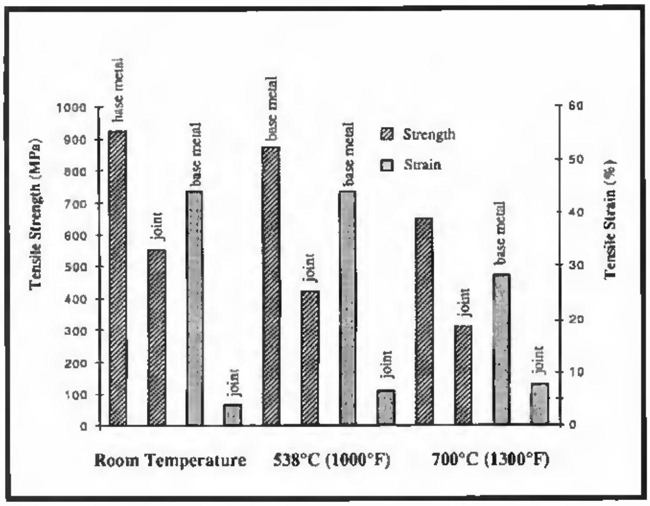

Fig. 5 — Results from tensile tests on the joints infiltrated by Ni-P eutectic at 980°C for 60 min. The powder interlayer was Ni-20Cr and the overall phosphorus content in each joint was 1.8 wt-%.

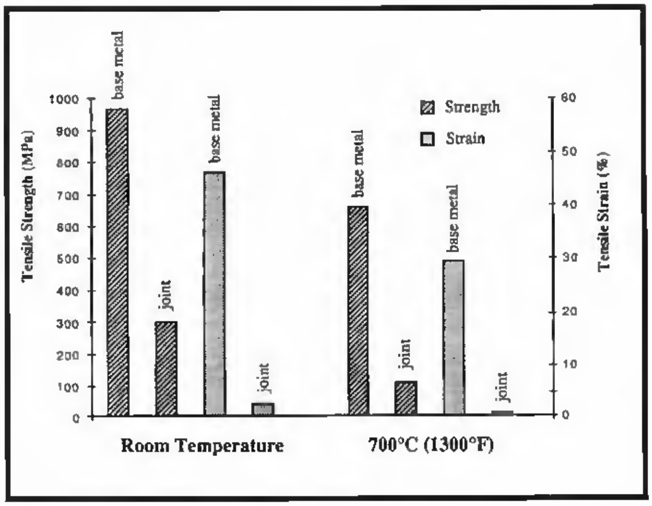

Fig. 6 — Results from tensile tests on the joints infiltrated by Ni-B eutectic at 1125°C for 60 min. The powder interlayer was Ni-20Cr and the designed boron content in each joint was 0.33 wt-%.

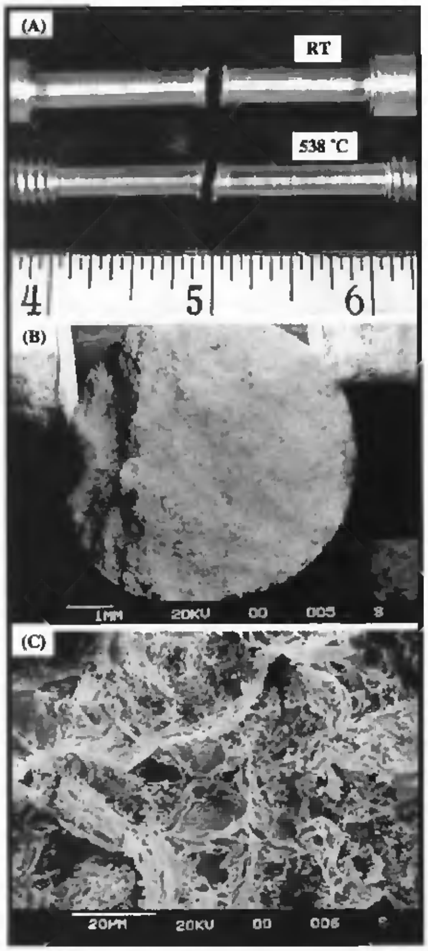

Fig. 7 — Fracture appearance of Ni-P eutectic infiltrated Ni-20Cr powder interlayer joints. A — Specimens showing fracture in the powder interlayers. B — Fracture surface of the sample tested at room temperature. C — Same as B, showing some oxides in the interlayer.

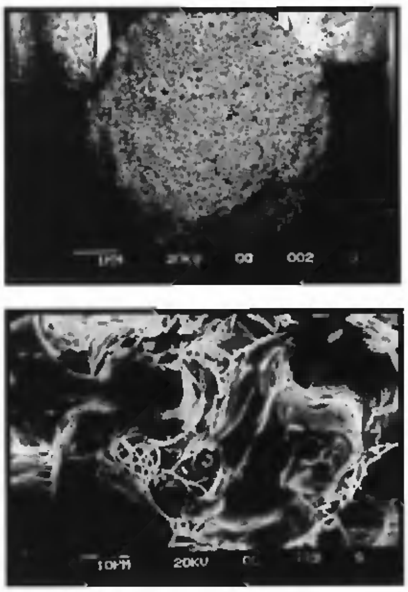

Fig. 8 — Fracture surface of the Ni-B eutectic infiltrated joint. The powder interlayer was Ni-20Cr and the boron content in the joint was about 0.33 wt-%. Residual porosities can be seen from the photographs.

of the residual voids. Figure 8 depicts the fracture appearance of the sample tested at room temperature. Residual pores can be seen from both of the metallographs.

Conclusions

In this study, the LIPB process was investigated for high temperature brazing of joints with large clearances. Calculations based on a binary eutectic system show that the volume fraction of residual porosity in the interlayer depends on the initial relative density of the interlayer, the shrinkage factor *k*, and the solubility of MPDs in the powder material. Ni-P and Ni-B eutectics and MBF-1006 (Ni-41.2Pd-8.8Si) were used as infiltrants, nickel and Ni-20Cr were used as powder interlayers to join nickel and Inconel 625 nickel-based alloys. The following results were obtained:

1) Brazements with large joint clearances could be made by the LIPB process, using Ni-P and Ni-B eutectics as the infiltrants. Intermetallic compounds were greatly decreased because of much smaller amount of phosphorus or boron contained in these joints, compared to those joined with commercial brazing alloys.

2) Ni-P eutectic was found to cause shrinkage of the nickel-based powder interlayer ($k<1$), and contribute to elimination of residual pores in the joint, whereas Ni-B eutectic showed less benefit in this regard.

3) Infiltration using MBF-1006 as the infiltrant was slow due to high solubility of palladium and silicon in the nickel-based powder interlayer. A proper mixture of the infiltrant and the interlayer is important to produce a fully infiltrated joint.

4) Tensile tests showed 60% joint efficiency up to 700°C when Inconel 625 was the base metal and Ni-P eutectic was the infiltrant. Plastic deformation was observed, though the ductility of the joint was still much lower than that of the base metal. Joints infiltrated by Ni-B eutectic

revealed poor tensile strength due to isolated pores in the interlayers.

Acknowledgment

The authors would like to thank the National Science Foundation (NSF) for supporting this research under contract number DMR-9301444.

References

1. Manente, D. 1993. Brazing of heat-resistant alloys, low-alloy steels and tool steels. *ASM Handbook, Welding, Brazing, Soldering*, 6: 924–930.

2. Humpston, G., and Jacobson, D. M. 1993. *Principles of Soldering and Brazing*, pp. 47–50. ASM Publication.

3. Sakamoto, A., Fujiwara, C., Hattori, T., and Sakai, S. 1989. Optimizing processing variables in high temperature brazing with nickel-based filler metals. *Welding Journal* 68(3): 63–71.

4. Schwartz, M. M. 1987. *Brazing*, pp. 131–187, ASM Publication.

5. Lugscheider, E., and Krappitz, H. 1986. The influence of brazing conditions on the impact strength of high temperature brazed joints. *Welding Journal* 65(10): 261-s to 267-s.

6. Lugscheider, E., Partz, K.-D., and Lison, R. 1982. Thermal and metallurgical influences on AISI 316 and Inconel 625 by high temperature brazing with nickel-based filler metals. *Welding Journal* 61(10): 299-s to 333-s.

7. Pattee, H. E. 1980. *Source Book on Brazing and Brazing Technology*, pp. 17–63. ASM Publication.

8. Duvall, D. S., Owczarski, W. A., and Paulonis, D. F. 1974. TLP bonding: A new method for joining heat resistant alloys. *Welding Journal* 53(4): 203–214.

9. Duvall, D. S., *et al.* 1972. Methods for diffusion welding the superalloy Udimet 700. *Welding Journal* 51(2): 41-s to 49-s.

10. Hoppin, G . S. III, and Berry, T. F. 1970. Activated diffusion bonding. *Welding Journal* 49(11): 505-s to 509-s.

11. Owczarksi, W. A., King, W. H., and Duvall, D. S. 1970. *Diffusion welding of the nickel-based superalloys*, U.S. Patent #3530568.

12. Liu, S., Olson, D. L., Martin, G. P., and Edwards, G. R. 1991. Modeling of brazing process that use coatings and interlayers. *Welding Journal* 70(8): 207-s to 215-s.

13. MacDonald, W. D. 1993. *Kinetics of transient liquid phase bonding*. Ph.D. thesis, Massachusetts Institute of Technology, Cambridge, Mass.

14. Zhuang, W. D. 1997. *Applications of metal powders for large gap joining*. Ph.D. thesis, Massachusetts Institute of Technology, Cambridge, Mass.

15. Riedel, W. 1991. *Electroless Nickel Plating*, pp. 9–29. Co-published by Finishing Publications and ASM International.